The Thick and Thin of Burning Nano-clay-nylon Composites

XIN LIU[2] and J.G. QUINTIERE[1]
[1]. Department of Fire Protection Engineering
University of Maryland
College Park, MD
[2] Underwriters Laboratories
Northbrook, IL

ABSTRACT

The flammability properties of pure Nylon 6 and clay additives of 2 and 5% in thicknesses ranging from 1.6 to 24 mm were examined. Data were obtained over a range of radiant heat fluxes (17 to 55 kW/m^2). The heats of combustion did not change with loading, and were 28 +/- 1 kJ/g. The critical heat flux for ignition also did not significantly change as it decreased from 17.7 to 16.0 for pure nylon to 5% clay addition. However, the addition of the clay could increase the ignition time by 30 to 100% over the pure nylon. This is believed to be due to the increased char residue and decrease in mass loss rate accordingly. The residual char-like yield was nearly identical to the clay loadings. The overall average mass loss rate was reduced by up to 50% for 5% clay over pure nylon for a given heat flux and thickness. For the clay nano-composites, the average burning rate increased as the thickness decreased. A theoretical model qualitatively explains the effect of thickness.

KEYWORDS: nylon clay-nano-composites, flammability, thermally thick and thin

NOMENCLATURE

a_p	pre-exponential factor	**Greek**	
c_p	specific heat (J/gK)	ε	emissivity
E	activation energy (J/mole-K)	ρ	density
h	enthalpy (kJ/g)	δ_s	thermal depth (mm)
Δh_c	heat of combustion (kJ/g)	**subscripts**	
Δh_{vap}	heat of vaporization (kJ/g)	a	active
k	thermal conductivity (W/mK)	c	char
$k\rho c$	thermal inertia (kW/m^{2}K)^{2}s)	cr	critical
l	sample thickness (mm)	d	decomposition
L	heat of gasification (kJ/g)	ext	external
m	mass (g)	i	incident
M	molecular weight	ig	ignition
q	heat (J)	g	gas
t	time (s)	**superscripts**	
T	temperature (K)	$\dot{X}$	per unit time

FIRE SAFETY SCIENCE–PROCEEDINGS OF THE EIGHTH INTERNATIONAL SYMPOSIUM, pp. 647-658

x	dimension into sample (mm)	X''	per unit area
X_c	char fraction (%)	X'''	per unit volume

INTRODUCTION

Composites consisting of nylon (PA-6) with small additives of montmorillonite (MMT) clay have shown significant improvements in many properties. For example, Giannelis [1] reports that an increase in thermal stability and a decrease in permeability can also be achieved by the addition of clay. The objective of this study is to determine the effects of clay loading on flammability properties, and to address the effect of thickness that has been evident in previous work by Gilman et al. [2]. They found that peak heat release rates per unit area were significantly reduced by adding clay. But these peaks were influenced by the sample thickness (8 mm) due to an insulated back-face, as the peaks occurred late in the burning period. In contrast, a thicker sample at 25 mm for pure nylon at the same heat flux showed an early peak plateau during steady burning of about 600 kW/m^2 compared to 2000 kW/m^2 at 8 mm [3]. Therefore, thickness effects are interfering with an independent assessment of the role of the clay agent. Yet reductions in burning rate stem from the formation of a char-like thermal barrier formed by the clay [4] although others suggest intermolecular effects with the clay as responsible [5].

This paper will examine the experimental results as a function of thickness in terms of a modeling framework. The modeling follows work of Staggs [6] and our previous studies on wood burning [7,8]. The experimental work aims to examine macroscopic bulk properties of flammability in order to obtain insight on the role of the nano-clay. These properties include the heat of combustion, critical heat flux for ignition and the deduced ignition temperature, thermal inertia, $k\rho c$, and the effective heat of gasification, L.

EXPERIMENTS

Experiments for the nano-composite materials were performed using the Cone Calorimeter. Thickness of the samples ranged over 1.6, 3.2, 4, and 8 mm, and several at 24 mm. The incident radiant heat fluxes ranged from the minimum needed for ignition to about 60 kW/m^2. Samples consisting of 75 mm diameter disks of pure Nylon 6 (polyamide 6), Nylon with 2% and 5% nano-clay additives were used. Their molecular properties are described more fully by Kashiwagi et al. [4]. Typical burning behavior is shown for pure nylon and 5% clay additive in Fig. 1.

Observations

Under high heat fluxes (above 30 kW/m^2), the pure Nylon sample exhibits a melting-like behavior and burns like a liquid. Under low heat fluxes, the surface appears to oxidize, and then forms a thin carbonaceous skin. For samples with clay, the time to ignition is increased as the clay loading is increased. This is likely due to a carbonaceous skin that is always formed before ignition. For high heat flux, at about 50 kW/m^2, the char-skin is relatively thin and weak and easily allows evaporated fuel gas to flow through. Consequently, flaming ignition is fairly uniform over the surface. For lower heat fluxes (less than 30 kW/m^2), the char skin is thicker and stronger, and trapped gases promote a bubble-like shell. Ignition occurs at small breaks in the char bubble, and the bubble collapses as full flaming commences. However, the char remains throughout the burning process.

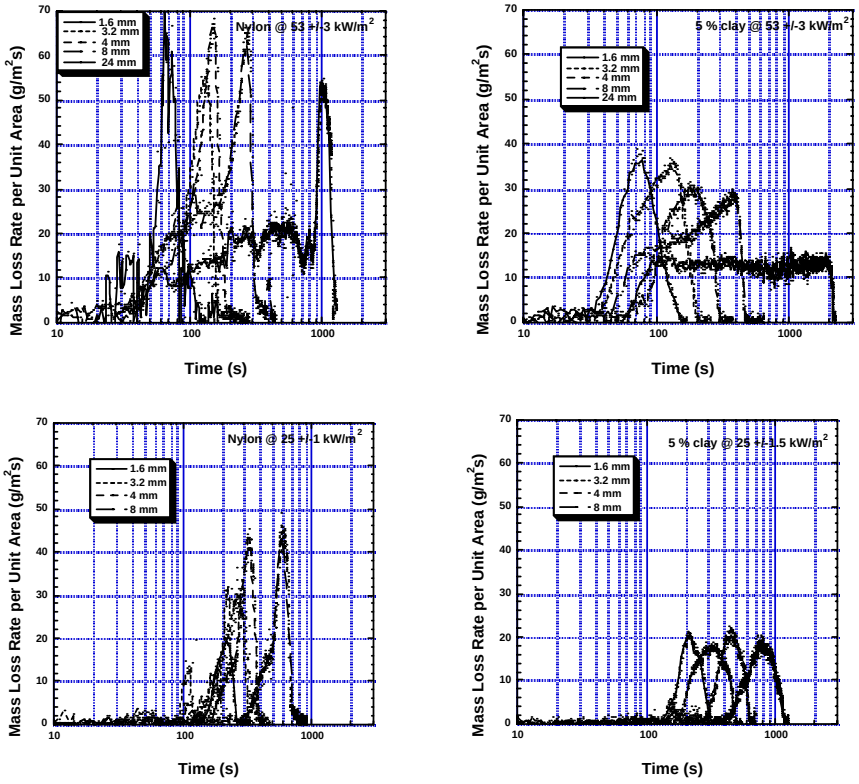

Fig. 1. The effect of heat flux and thickness for nylon and 5% composite samples.

Samples consisting of different clay additives have different amounts of residue. For pure Nylon, none is left after burning. For Nylon with 2% clay, at the end of burning, the char skin remains, but it is nearly hollow between the top char skin and the bottom of the aluminum cup. For nylon with 5% clay, the residue is more uniformly distributed. The thesis by Liu [9] contains more details on these observations and on the data to follow.

Measurement Results

Primarily, the pure nylon and 5% clay samples will be compared. Property data were analyzed based on the full flaming period and on the peak average conditions associated with either the first or second burning peaks as indicated in Fig. 1.

The heats of combustion were essentially invariant, and the averages over all the thicknesses are shown in Fig. 2. Essentially, the gaseous fuel coming off all samples is the same fuel. The char residue fraction (Fig. 3) was found to be almost coincident with the clay loading, and hence this implies the char is essentially the clay residue.

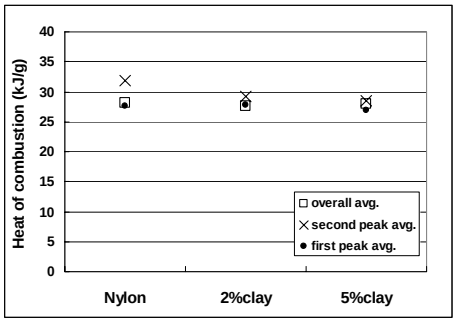

Fig. 2. Heats of combustion.

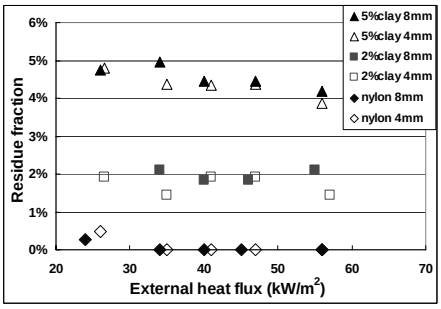

Fig. 3. Residue fraction.

The heat of gasification depends on what burning period it is determined from, as it is defined by $L = \dot{q}''_{net} / \dot{m}''$. Figure 4 shows well-behaved data based on the overall average burning rate for the nylon only. All of the samples exhibited similar linear behavior. However, the corresponding values computed from the slopes ranged from about 1.5 to 4 kJ/g and only showed a slight tendency to increase with clay loading and thickness. Hence, *L* does not easily explain the differences in the peak burning rates. Reductions with the clay are more due to the reduction in the net flame heat flux.

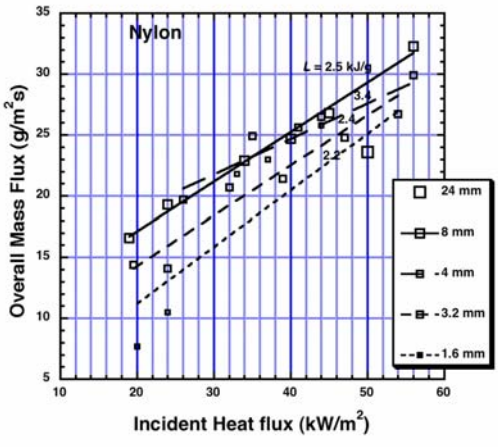

Fig. 4. Heat of gasification for nylon.

Ignition behavior generally followed thick solid behavior with the time to ignite inversely varying with the square of the heat flux. However, shorter ignition times occurred for thinner samples. Results for the 5% clay composite are shown in Fig. 5. The critical flux for ignition was slightly lower for the clay additive, but the ignition times were increased by up to a factor of 2 for the 5% additive over the pure nylon. Table 1 gives a summary of the ignition and other properties deduced from the Cone data.

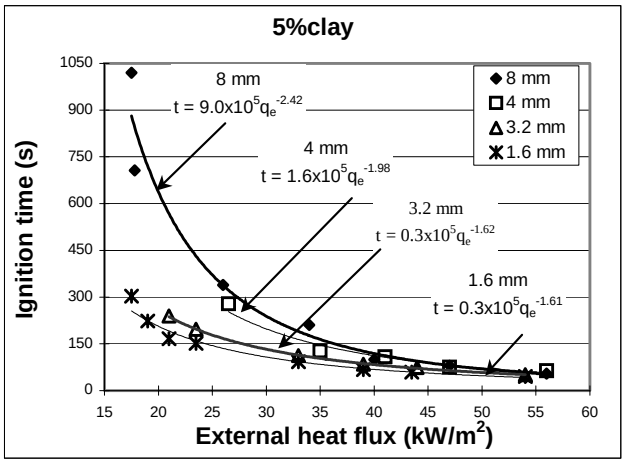

Fig. 5. Ignition of 5% clay samples.

Table 1. Summary of effects on ignition and burning.

Material	"Char" residue %	$k\rho c$ $(kW/m^2K)^2s$	Critical Flux (kW/m^2)	Heat of Combustion (kJ/g)	Heat of Gasification (kJ/g)
Nylon	0 - 0.5	0.7 – 0.8	17.7	27 - 29	1.5 – 3.5
2 % clay	2	1.1 – 1.5	17.5	27 - 29	1.5 – 4.0
5 % clay	4 - 5	1 – 1.5	16.0	27 - 29	2.5 – 3.5

ANALYSES

The current study sought to investigate the effect of thickness and heat flux on the burning and ignition behavior for pure nylon and its nano-composites of 2 and 5% clay. The principal effect of the clay has been the formation of a "char-like" residue that inhibits heat flow and therefore reduces the burning rate. It should be pointed out that this "char" residue is small compared to wood that can vary from 20 to 40% [7].

It will be shown that two mechanisms are responsible for the burning rate behavior. One is based on heat transport into the solid that is absorbed into the heat of vaporization or decomposition of the material. The other is based on the kinetics of decomposition. The first applies to thick samples before the heating wave reaches the back-face of the sample. The second, the kinetic process, occurs for thin samples that have been sufficiently preheated. The back-face effect in an insulated sample is also another example where kinetic effects dominate. In the kinetics-controlled case, the material tends to heat more uniformly during decomposition. In the heat conduction case, a sharp temperature gradient exists at the decomposition front. These thermal features are illustrated in Fig. 6.

Burning Rate Model

The burning rate model is based on the decomposition model used by Boonmee [8] for wood. The model will not be fully developed here. Its results will help to explain the burning behavior of the samples without obtaining a direct solution.

The model considers the decomposing solid as a perfect mixture of original solid fuel (active species, a), and char c)). The char forms a layer, filling the same volume of the original material. If no char is produced, the heated surface simply regresses. Gaseous fuel is generated within, and flows without resistance through the solid. The gas has negligible mass in the solid mixture. Decomposition is given in terms of an Arrhenius first order chemical reaction. The chemical equation is given as follows:

1 g active (original) solid $\rightarrow X_c$ g char + (1- X_c) g gaseous fuel. (1)

Conservation of mass is derived for a differential (1-D) element of solid fuel with the coordinate system given in Fig. 7. For the charring case, x is measured from its original position, but in the non-charring case, it is measured from the regressing surface. Details of the derivations are not shown. The mixture density is given as $\rho = \rho_a + \rho_c$ and the local mass flux is $\dot{m}''_g(x)$. The conservation of mass becomes

$$\frac{\partial \rho}{\partial t} = \frac{\partial \dot{m}''_g}{\partial x}. \quad (2)$$

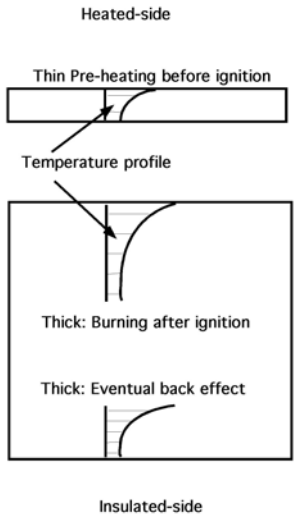

Fig. 6. Thin and thick effects.

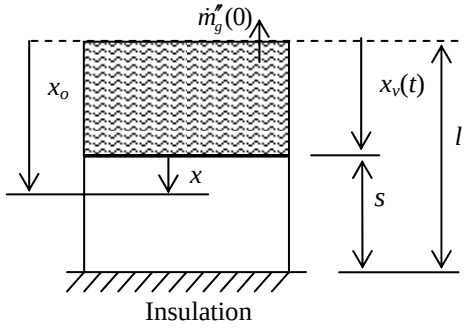

Fig. 7. Coordinate systems.

In the energy equation, gaseous fuel with enthalpy h_g leaves, and h is enthalpy of the active-char mixture. The enthalpies are taken in terms of the heats of formation of the

species. The energy equation for constant pressure conditions, with species enthalpy $h_i = \Delta h^o_{f,i} + h_{s,i}$, and sensible enthalpy, $h_{s,i} = \int_{25^oC}^{T} c_{p,i} dT$, can be written as

$$\frac{\partial(\rho h_s)}{\partial t} - \frac{\partial(\dot{m}''_g h_{s,g})}{\partial x} = \frac{\partial}{\partial x}(k\frac{\partial T}{\partial x}) + \frac{\Delta h_d}{(1-X_c)}\frac{\partial \rho}{\partial t} \tag{3}$$

where the heat of decomposition per unit of mass of original material at 25°C is

$$\Delta h_d \equiv -\left[\Delta h^o_{f,a} - X_c \Delta h^o_{f,c} - (1-X_c)\Delta h^o_{f,g}\right]. \tag{4}$$

Expanding the first term and substituting from the conservation of species, the first term of Eq. 3 can be written as:

$$\rho\frac{\partial h_s}{\partial t} + \frac{h_{s,a}}{(1-X_c)}\frac{\partial \rho}{\partial t} + \frac{h_{s,c}X_c}{(1-X_c)}\left(-\frac{\partial \rho}{\partial t}\right). \tag{5}$$

Further manipulations and converting sensible enthalpy to temperature gives

$$\rho c_p \frac{\partial T}{\partial t} - \dot{m}''_g c_{p,g}\frac{\partial T}{\partial x} = \frac{\partial}{\partial x}(k\frac{\partial T}{\partial x}) + \frac{\partial \rho}{\partial t}\frac{\Delta h_{vap}}{(1-X_c)} \tag{6}$$

where a heat of vaporization is defined to account for the chemical and phase changes at the decomposition temperature, T_v,

$$\Delta h_{vap}(T_v) = \Delta h_d - h_{s,a}(T_v) + X_c h_{s,c}(T_v) + (1-X_c)h_{s,g}(T_v). \tag{7}$$

Note, if there is no chemical decomposition and no char, only a vaporization phase-change from solid (a) to gaseous fuel (g) occurs, then $\Delta h_{vap}(T_v) = h_{s,g}(T_v) - h_{s,a}(T_v)$, the thermodynamic heat of vaporization for a phase change from a solid to a gas.

The conservation of energy for a non-charring material with chemical decomposition and surface regression is similarly found, but with a moving coordinate system as shown in Fig. 7. It becomes

$$\rho c_p \frac{\partial T}{\partial t} - c_p \dot{m}''_g(0)\frac{\partial T}{\partial x} - \dot{m}''_g c_{p,g}\frac{\partial T}{\partial x} = \frac{\partial}{\partial x}(k\frac{\partial T}{\partial x}) + \frac{\partial \rho}{\partial t}\frac{\Delta h_{vap}}{(1-X_c)}. \tag{8}$$

Solutions

From Eqs. 6 and 8, the form of a solution can be expressed that reveals the qualitative behavior of burning. The total mass flux due to a constant incident heat flux will be considered, and no changes due to flame heating are included.

Thermally Thick Solutions: Consider some appropriate assumptions for the thermally thick case. Take Δh_{vap} constant at a thin reaction region where T_v is uniform. This will apply for rapid decomposition under high heating rates. It can be shown for the charring case by integrating over $0 \le x \le l$, that

$$\dot{m}''_g(0) = \left(\dot{q}''_i - \sigma T^4(0) - \int_0^l \rho c_p \frac{\partial T}{\partial t} dx \right) / \left(\frac{\Delta h_{vap}}{(1 - X_c)} + c_{p,g}(T(0) - T_v) \right), \tag{9}$$

and for the non-charring case:

$$\dot{m}''_g(0) = \left[\dot{q}''_i - \sigma T_v^4 - \int_0^s \rho c_p \frac{\partial T}{\partial t} dx \right] / L \text{ where } L \equiv \left[\Delta h_{vap} + + c_p (T_v - T(s)) \right]. \tag{10}$$

Here, L is the traditional heat of gasification as a property. It is seen from these solutions that the build up of char will cause an increase in the surface temperature over the temperature of decomposition. This increase will cause more heat loss from the sample that will diminish the burning rate as time increases. The char reduction factor ($1-X_c$) will also decrease the mass loss over a comparable non-charring material. Spearpoint and Quintiere [7] have shown that for wood, the charring mass loss rate will follow a $t^{-1/2}$-behavior after an initial peak.

Thermally Thin Solution: For a thermally thin material, the temperature would ideally be uniform throughout, and Eqs. 6 and 8 apply without the variations in x. During burning, the vaporization temperature has been taken as constant in the thermally thin region. From Eq. 2 and a first-order Arrhenius reaction rate

$$\frac{\partial \rho}{\partial t} = -\rho_a a_p e^{-\frac{E}{RT}} \tag{11}$$

it follows that the mass flux at the surface is

$$\dot{m}''_g(0) \approx \rho_a a_p e^{-E/RT_v} \cdot l_{thin} \tag{12}$$

where l_{thin} can be the sample thickness from the start of burning, or it can be a region near the back-face when the thermal wave arrives. It should be recognized that the active density would not be constant over this burning period as it is depleted, and hence Eq. 12 is approximate. The maximum or initial value gives a measure of the mass flux for the thin case. For TGA data of nylon it was found that a_p = 1.1 x 10^{19} and E = 2.4 x 10^5 J/mole-K [10]. The result, for a peak vaporization temperature of about 425°C, is 13.3 kg/m^{2}s, and for an onset vaporization temperature of 350°C, 95 kg/m^{2}s for a thickness of 1 mm. This shows the potentially high values for the thermally thin case, but they would be mitigated by the decrease in the active fuel. The form of the solution shows that the thin domain will give a sudden peak followed by a rapid decrease in the

mass flux. This behavior is characteristic of the physical thinness of the sample, and those that are heated more slowly as seen in Fig. 2.

Criteria for Thermally Thick and Thin Burning

The thickness of the reaction zone in the thin case depends on two effects. First, during the heating to ignition, the back-face of the sample could have the thermal wave reach it at ignition. The material would have behaved as thermally thick for ignition, but now the burning is occurring with the sample fully heated at the start. Secondly, the sample could be thermally thick during most of the burning following ignition, but the thermal wave during burning eventually reaches the back-face. The depths of these thermal layers indicate the magnitude of the reaction zone in thermally thin burning.

Thermally Thin at Ignition: Spearpoint and Quintiere [7] report an approximate solution for ignition in terms of a thermal depth. The thermal depth at the time of ignition is set equal the sample thickness to give the end of the thermally thick heating behavior period. The criterion for burning as a thin sample is then found to be

$$l_{thin} \le 2\frac{(T_{ig} - T_o)k}{\dot{q}_i''} \tag{13}$$

Here the incident heat flux is the external radiant flux. If the temperature at the onset of degradation is used, then it can be estimated for the nylon samples that

$$l_{thin}(\text{mm}) \approx \frac{2(325^oC - 25^oC)(0.2\times10^{-3}\ \text{kW/mK})}{\dot{q}_i''(\text{kW/m}^2)} \approx \frac{120}{\dot{q}_i''(\text{kW/m}^2)} \tag{14}$$

This suggests samples of 2 to 6 mm could act as thermally thin immediately following ignition. Figure 8 shows an example of burning 3.2 mm thick nylon at different heat fluxes. For the higher heat fluxes, steady burning is clearly indicated, but for the lowest flux, a thermally thin behavior is seen. This dependence on heat flux is clearly seen in the criterion. Also shown, by the high heat flux curves, is the thermally thin burning behavior that occurs when the back-face begins to be heated.

Back-face Thermally Thin Effect: As the degradation progresses in a sample of original thickness, *l*, a thermal depth will advance from the vaporization region as illustrated in Fig. 6. Eventually it will reach the back-face. At that point for an insulated back surface the temperature will increase over the steady solution within the thermal depth region and kinetic effects will proceed to control the burning rate. For a thick sample, the thermal depth will reach a constant value during steady burning. Hopkins and Quintiere [3] give this steady depth as

$$\delta_s = \frac{2kL}{c(\dot{q}_i'' - \sigma T_v^4)}. \tag{15}$$

Staggs [6] obtains a similar result, in our terminology, as $\delta_s = 2k(T_v - T_o)/(\dot{q}_i'' - \sigma T_v^4)$. From Fig. 7, this transition to thermally thin burning will occur when

$$l = x_v + \delta_s \tag{16}$$

for steady burning in a non-charring material. Under these conditions, the regression front is given from Eq. 10 as

$$x_v = \frac{\dot{m}''_g}{\rho_o} t = \left(\dot{q}''_i - \sigma T_v^4\right) t / \rho_o L \tag{17}$$

where t is the time to reach the back-face. This vaporization distance is the dominant distance factor for thick samples in indicating when the back-face effect occurs. The smaller thermal depth appears to be not so important. All of the data, including the charring samples are plotted as $\dot{q}''_i t$ versus l in Fig. 9. It does a good job of representing all but the small thicknesses. Although charring materials, from Spearpoint and Quintiere [7], would indicate that the vaporization front and the thermal depth both are a weak function of the heat flux and grow as $\sqrt{kt/\rho c}$, this trend is not seen for the weakly charring clay nano-composites in Fig. 9. Perhaps higher char yields would produce this indicated charring behavior. The initial thermally thin regions, for small l values, have been estimated and shown in Fig. 9 from the thin-thickness ignition criterion. From Eq. 17, the slope of the linear data fits allows a computation for a heat of gasification. For density of 1108 kg/m^3, the L values are 1.88, 2.38 and 2.71 kJ/g for 0, 2 and 5% clay. These are not unreasonable in view of Table 1.

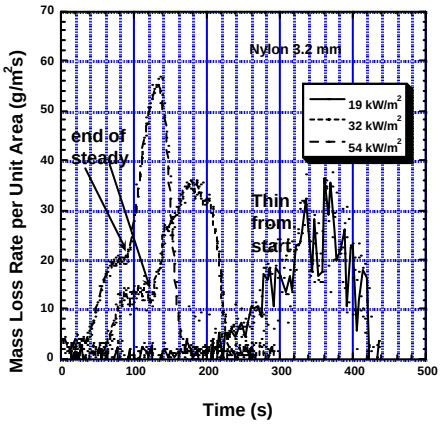

Fig. 8. Thick and thick behavior.

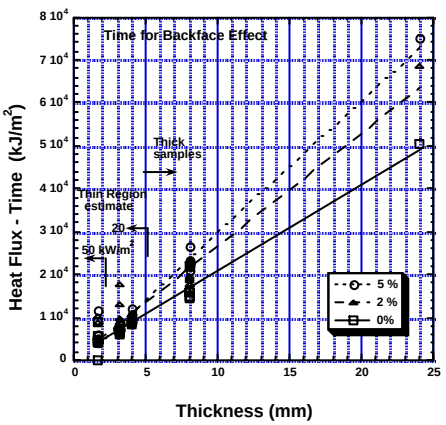

Fig. 9. Back face thermal depth time.

Overall Burning Behavior and the Effect of Thickness

The two-kinds of burning behavior – thick and thin – make it difficult to describe the effect of the nano-clay addition to nylon in a universal way. It is clear that the weak char residue of the clay is the principal factor in reducing the burning rate for the thick samples as the char accumulates. However, the thermally thin burning behavior, and its dependence on both char yield and kinetic properties, is another factor. It is well known for wood sticks, the burning rate per unit area varies as $l^{-0.5}$ where l is the stick diameter.

In general, the heat flux should also be a factor, roughly in a linear fashion. Therefore, an empirical power-law might in the form:

$$\dot{m}''(\mathrm{g/m^2s}) = C\dot{q}_i''(\mathrm{kW/m^2})l^n(\mathrm{mm})\,. \tag{18}$$

Figure 10 includes all of the data plotted in this fashion with C = 0.52 for nylon, 0.61 for 2 %, and 0.52 for 5%; and n = + 0.095 for nylon, - 0.11 for 2% and – 0.17 for 5%. Figure 10 shows that there can be as much as a 50% reduction in burning rate for the addition of 5% nano-clay compared to nylon for a given heat flux and thickness. It also shows that the clay additive has an effect similar to the char on wood.

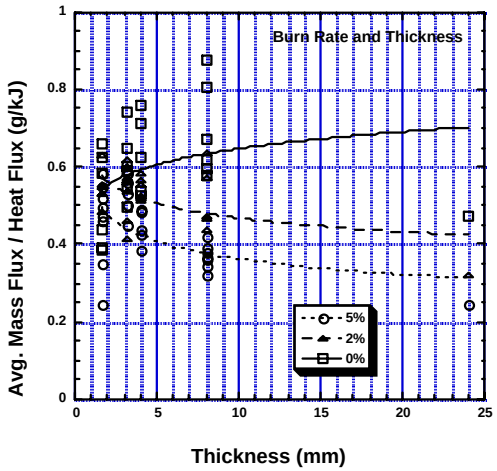

Fig. 10. Thickness effect on burning.

CONCLUSIONS

The clay nano-additive significantly increases the ignition time and reduces the burning rate of pure nylon. This is primarily associated with the formation of a char. Thickness effects on burning are described in terms of thermally thin and thick behavior. The average burning rate is seen to depend on the incident heat flux and inversely on thickness for the clay containing composites that is indicative of char layer insulation. The gaseous fuel produced is that associated with the nylon and has no change in its heat of combustion.

ACKNOWLEDGEMENTS

The FAA under Richard Lyon sponsored this work and that support is greatly appreciated. T. Kashiwagi supplied the samples and significant information on TGA and thermal property data.

REFERENCES

[1] Giannelis, E.P., “Polymer Layered Silicate Nanocomposites,” *Advanced Materials*, **8**, pp. 29-35, (1995).

[2] Gilman, J.W., Kashiwagi, T., Morgan, A.B., Harris, R.H., Brassell, L., and Van Landingham, C.L.J.M., "Flammability of Polymer Clay Nanocomposites Consortium: Year One Annual Report. 2000," National Institute of Standards and Technology, Gaithersburg, MD, 2000.

[3] Hopkins, D., and Quintiere, J.G., "Material Fire Properties and Predictions for Thermoplastics," *Fire Safety Journal*, **26**, pp. 241-268, (1996).

[4] Kashiwagi, T., Harris, R.H., Zhang, X., Briber, R.M., Cipriano, B.H., Raghavan, S.R., Awad, W.H., and Shields, J.R., "Flame Retardant Mechanism of Polyamide 6-Clay Nanocomposites," *Polymer*, **45**, pp. 881-891, (2004).

[5] Jang, B.N., and Wilke, C.A., "The Effect of Clay on the Thermal Degradation of Polyamide 6 in Polyamide 6/Clay Nanocomposites," *Polymer*, **46**, pp. 3264-3274, (2005).

[6] Staggs, J.E.J., "A Theory for Quasi-steady Single-Step Thermal Degradation of Polymers," *Fire and Materials*, **22**, pp. 109-118, (1998).

[7] Spearpoint, M.J. and Quintiere, J.G., "Predicting the Burning of Wood Using an Integral Model," *Combustion and Flame*, **123**, pp. 308-324, (2000).

[8] Boonmee, N., and Quintiere, J.G., "Glowing and Flaming Auto-Ignition of Wood," *Proc. of the Combustion Institute*, **30**, pp. 2303-2310, (2004).

[9] Liu, Xin, "Flammability Properties of Clay-Nylon NanoComposites," M.S. Thesis, Dept. of Fire Prot. Engrg., University of Maryland, College Park, 2004.

[10] Kashiwagi, T., Private Communication: Thermal Properties and TGA Data for Nylon and Nylon+5%clay With a Series of Constant Heating Rates, 2004.